2006

Spectroscopic ellipsometry and absorption study of Zn1-xMnxO/Al2O3 (0 <= x <= 0.08) thin films

Ghil Soo Lee
Kyunghee University

Ho Suk Lee
Kyunghee University

Tae Dong Kang
Kyunghee University

See next page for additional authors

Spectroscopic ellipsometry and absorption study of $Zn_{1-x}Mn_xO/Al_2O_3$ ($0 \leqslant x \leqslant 0.08$) thin films

Ghil Soo Lee, Ho Suk Lee, Tae Dong Kang, and Hosun Lee[a)]
Department of Physics, Kyung Hee University, Suwon 446-701, Korea

C. Liu, B. Xiao, Ü. Özgür, and H. Morkoç
Department of Electrical Engineering, Virginia Commonwealth University, Richmond, Virginia 23284

(Received 19 December 2005; accepted 10 March 2006; published online 15 June 2006)

We grow $Zn_{1-x}Mn_xO/Al_2O_3$ ($0 \leqslant x \leqslant 0.08$) thin films on sapphire (0001) using radio-frequency sputtering deposition method with Ar and various N_2 flow rates. We examine the effect of N_2 codoping on the band gap and Mn-related midgap absorption of (Zn,Mn)O. Using spectroscopic ellipsometry, we measure pseudodielectric functions in the spectral range between 1 and 4.5 eV. Using the model of Holden *et al.* [T. Holden *et al.*, Phys. Rev. B **56**, 4037 (1997)], we determine the uniaxial (Zn,Mn)O dielectric function and the E_0 band-gap energy. The fitted band gap does not change appreciably with increasing Mn composition up to 2%. We find a very large broadening of both the E_0 band gap and its exciton partner E_{0x} peaks even for less than 2% of optically determined Mn composition. In ellipsometric spectra, we also find Mn-related 3 eV optical structure. In particular, optical absorption spectra with varying N_2 gas flow rate show that the Mn-related peak intensity decreases with increasing N_2 flux. The decrease of the 3 eV Mn-related peak intensity is attributed to increasing N_2 flow rate and Mn–N hybridization. © *2006 American Institute of Physics*. [DOI: 10.1063/1.2202097]

I. INTRODUCTION

Diluted magnetic semiconductor (DMS) material has a promising application in spintronics. In this application, we focus on spin degree of freedom rather than electron charge in electronic devices. III-V and II-VI semiconductors with transitions metals are widely investigated for the spintronic applications. DMS is a type of semiconductor in which magnetic transition-metal ions replace a fraction of cations of the host semiconductor material. Based on the prediction of Dietl *et al.*,[1] (Zn,Mn)O has been the focus of considerable research efforts[2–5] to achieve reliable ferromagnetic DMS with a Curie temperature (T_C) well above room temperature. (Zn,Mn)O has been predicted to be antiferromagnetic but changes to ferromagnetic if it is codoped with N, where N serves as a *p*-type dopant.[6] Reliable *p*-type doing of ZnO, however, remains a challenge due to the intrinsic *n*-type defects such as Zn interstitials or O vacancies in ZnO. As, P, and N have been used in the attempts to realize *p*-type ZnO, and recently there has been success in achieving *p*-type conductivity using nitrogen dopant.[7,8]

In this work, (Zn,Mn)O thin films were prepared with and without GaN buffer layers by using rf sputtering deposition in a gas mixture of Ar and N_2. Using optical absorption method, we measured the optical gap energy, i.e., band-edge energy, and thereby estimated the Mn composition. Using spectroscopic ellipsometry, we measured the pseudodielectric functions of (Zn,Mn)O. Using the model of Holden *et al.*, we fitted the dielectric function and determined the band-gap parameters as a function of Mn composition. We also found a broad 3 eV peak which was attributed to intra-*d*-shell transitions of Mn^{2+} ions from both ellipsometric and optical absorption data.

II. EXPERIMENTS

(Zn,Mn)O thin films of ~0.5 μm thickness are deposited on (0001) sapphire substrate with/without 2-μm-thick GaN buffer layers by rf magnetron cosputtering of ZnO and Mn targets.[9] A gas mixture of N_2 and Ar is used as the sputtering ambient, so that N is supplied as active N species in the deposition process. The GaN templates are grown on *c*-plane sapphire substrates by metal-organic chemical-vapor deposition (MOCVD). The (Zn,Mn)O films are deposited at a substrate temperature of 500 °C. The flow rate of Ar is kept at 60 SCCM (SCCM denotes cubic centimer per minute at STP) in all the experiments, and the flow rate of N_2 is varied from 0 to 15 SCCM. A rf power of 100 W and a dc power of 10 W is applied to sputter the ZnO target and the Mn target, respectively. The targets are presputtered for 5 min before the actual deposition to remove any contamination from the target surface. The optical properties of the (Zn,Mn)O films are examined using optical absorption spectra at room temperature. We used a 20 W tungsten lamp, a 1250 mm monochromator, and a photomultiplier tube in photon counting mode. The beam was incident normally on the sample surface. The crystallographic properties of the thin films are investigated by high-resolution x-ray diffraction using a Cu $K\alpha$ source (Philips, X'Pert). We measured optical absorption spectra and determined the optical gap energy (band-edge energy). Compared to literature, we determined the Mn composition from the optical gap energy estimated from the optical absorption measurement. Using vari-

a)Author to whom correspondence should be addressed; electronic mail: hlee@khu.ac.kr

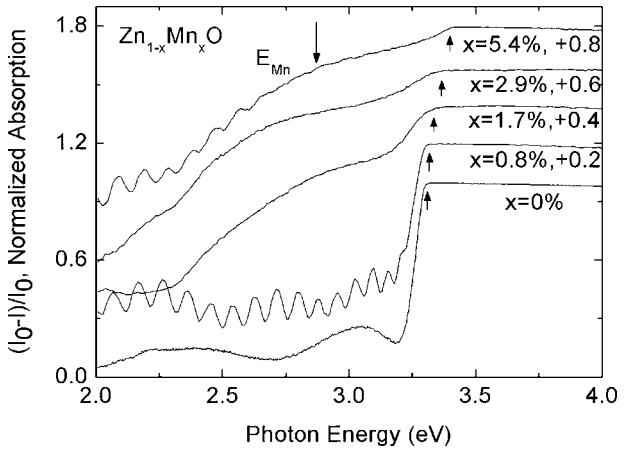

FIG. 1. Optical absorption spectra of $Zn_{1-x}Mn_xO$ thin films with $x=0$, 0.008, 0.017, 0.029, and 0.054. The arrows mark the optical band-gap energy and Mn-related peak, respectively. For simplicity, each spectrum was shifted vertically by +0.2, +0.4, +0.6, and +0.8, respectively.

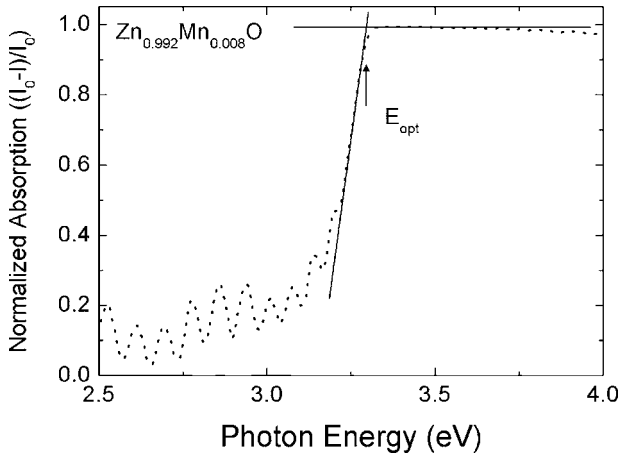

FIG. 2. Optical absorption spectra of $Zn_{0.992}Mn_{0.008}O$ thin film: An example of the determination of the optical gap.

able angle spectroscopic ellipsometry (VASE model, J. A. Woollam Inc.), we measured the pseudodielectric function of (Zn,Mn)O in the spectral range between 1 and 5 eV with angles of incidence 65°, 70°, and 75° at room temperature. The ellipsometric configuration was a rotating-analyzer-type with an autoretarder.

III. RESULTS AND DISCUSSION

Absorption spectra were taken at room temperature for all the (Zn,Mn)O thin films grown with different Mn compositions, and the optical gap was estimated. The Mn compositions were 0.0, 0.008, 0.012, 0.013, 0.014, 0.017, 0.023, 0.025, 0.029, 0.054, 0.057, 0.070, and 0.074. Part of the results are shown in Fig. 1. The strong oscillation below band gap is due to interference inside the 2-μm-thick GaN buffer layer. To obtain larger than 3% of Mn composition, we found that the GaN buffer layer was desirable to get high crystallinity. The lattice mismatch is much smaller for ZnO/GaN interface (1.8%) than for ZnO/Al_2O_3 (18%).[10]

Optical gap energy was estimated from the optical absorption spectra. In order to measure absorption spectra, we subtracted the intensity (denoted as I) of the transmitted beam with a sample on the mount from that with no sample (denoted as I_0). Therefore, $(I_0-I)/I_0$ designates the normalized absorption spectra. We used a cut-off filter ($\lambda=530$ nm) to remove the second-order effect of the luminescence from the (Zn,Mn)O samples due to the grating. Note that we designate the band-edge energy as optical gap energy, which was measured by using optical absorption spectroscopy, whereas the ellipsometrically determined gap is denoted as band-gap energy. In general, absorption increases dramatically near the optical gap energy. As is shown in Fig. 2, after drawing tangential lines below and above the band gap in the absorption spectra, we designated the intersection point as the optical gap assuming $\alpha \propto (E_{\text{opt}}-E)$ near the optical gap energy. The uncertainties were less than 3 meV. There are other phenomenological expressions for energy dependence of optical absorption spectra, for example, such as $\alpha^2 \propto (E_{\text{opt}}-E)$.[2] As long as one is consistent in estimating the optical gap energy, both methods are acceptable.

The Mn composition was estimated from the optical gap energy with the equation $E_{\text{opt}}(x)=3.280+1.930x-1.827x^2$(eV).[11] The above equation is very similar to that of Ref. 3, where (Zn,Mn)O thin films were grown on sapphire using by pulsed laser deposition (PLD) method. In our work, it was estimated from similar optical absorption data of the (Zn,Mn)O thin films grown by using peroxide molecular-beam epitaxy on sapphire substrate.[11] We neglected any strain effect on the band-gap energy. Therefore, our identification of Mn composition may not be exact. Actually Mn solubility depends on deposition method and conditions. Note that Fukumura *et al.*[2] obtained up to 36 mole % of Mn in wurzite-phase (Zn,Mn)O thin films which were grown by using PLD method. The optical gap energy of (Zn,Mn)O films prepared in this study increases to 3.41 eV as compared to that of the undoped ZnO film 3.280 eV. This increase of band-gap energy is mainly caused by Mn incorporation into ZnO lattice.

As compared to the absorption spectrum of undoped ZnO, another feature of the spectra of all (Zn,Mn)O layers is that they exhibit a broad and structureless midgap peak, which has been often reported from Mn-doped ZnO materials.[2,3,12] Using cathodoluminescence, Jin *et al.*[12] attributed the midgap peak to the overlap of the intra-*d*-shell transitions of Mn^{2+} from its ground state $^6A_1(s)$ to $^4T_1(G)$, $^4T_2(G)$, $^4A_1(G)$, and $^4E(G)$. These signatures of d-d^* transitions indicate that Mn is in the divalent state Mn^{2+} at the Zn site. The intensity of this midgap peak usually increases with Mn composition in ZnO.[2,3,12] Jin *et al.*[12] found that the midgap absorption strength per mole of Mn^{2+} increased substantially above Mn=0.055 and attributed the phenomenon to the formation of Mn–O–Mn clusters.

Absorption spectra were taken at room temperature for doped (Zn,Mn)O thin films grown with different N_2 flow rates, and the results are shown in Fig. 3. The absorption spectra show decreasing of the midgap absorption intensity at 3 eV with increasing N_2 flow rate. Therefore, in our study the Mn concentration in the film is lowered by introducing

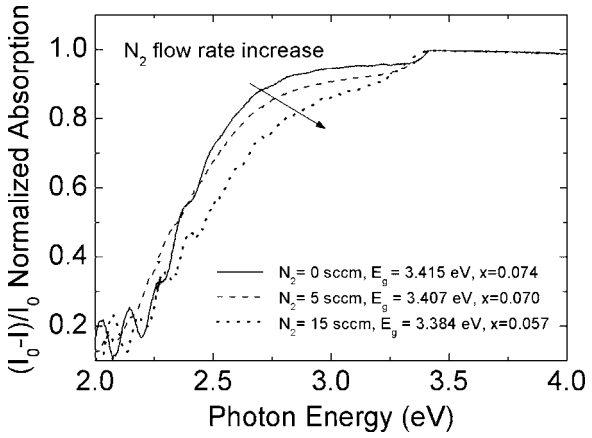

FIG. 3. Optical absorption spectra of $Zn_{1-x}Mn_xO$ ($x \approx 0.07$) thin film with varying nitrogen gas flow.

N_2 in the gas ambient. With increasing N_2 flow from 0 to 15 SCCM, the optical gap energy decreased slightly. The x-ray-diffraction peak of (002) of (Zn,Mn)O did not change with increasing N_2 gas flow, showing that the lattice parameter change was within experimental error. The decrease of Mn composition and consequent decrease of both optical gap energy and midgap peak intensity with increasing N_2 flow rate may be explained due to the decrease of Ar pressure with increasing N_2 flow rate. With increasing N_2 flow rate, the incorporation of Mn ions in ZnO matrix decreased and consequently optical gap energy decreased by up to 31 meV at 15 SCCM of N_2 flow rate. Another factor contributing to the decreasing 3 eV midgap absorption could be the hybridization between N 2*p* and Mn 3*d* electrons as was calculated by Wang *et al.*[6] The hybridization between N and Mn ions would suppress the d-d^* transitions in single-ion Mn^{2+} and would also suppress the formation of Mn–O–Mn clusters.

Selected (Zn, Mn)O thins films were measured using spectroscopic ellipsometry. Figure 4 shows the pseudodielectric function of (Zn,Mn)O ($x=0, 0.014, 0.017$) for the incidence angle of 70°. For simplicity, we did not show the pseudodielectric function for the incidence angles 65 ° and 75°. Here we only showed the pseudodielectric function spectra of (Zn,Mn)O thin films grown on sapphire without GaN buffer layers because multilayer modeling did not provide a good fit for the dielectric function of (Zn,Mn)O thin films grown with GaN buffer layer due to increased complexity. Figure 5 shows the fitted dielectric function of (Zn,Mn)O using uniaxial model for the thin films ZnO [Figs. 5(a) and 5(b)], $Zn_{0.086}Mn_{0.014}O$ [Figs. 5(c) and 5(d)], and $Zn_{0.083}Mn_{0.017}O$ [Figs. 5(e) and 5(f)].[4,13] The E_0 and E_{0x} peaks were overlapped due to substantial broadening of each peak. We modeled the pseudodielectric function as composed of (Zn,Mn)O layer, ZnO buffer layer, and sapphire substrate using the WVASE32 model software. We used the values of the dielectric function of sapphire from Ref. 14. We incorporated surface roughness assuming the surface layer as a mixture of (Zn,Mn)O top layer and voids. We neglected backside reflection because the back surface was rough. Since (Zn,Mn)O has a wurtzite structure and is uniaxial, we performed anisotropic modeling for the dielectric function.

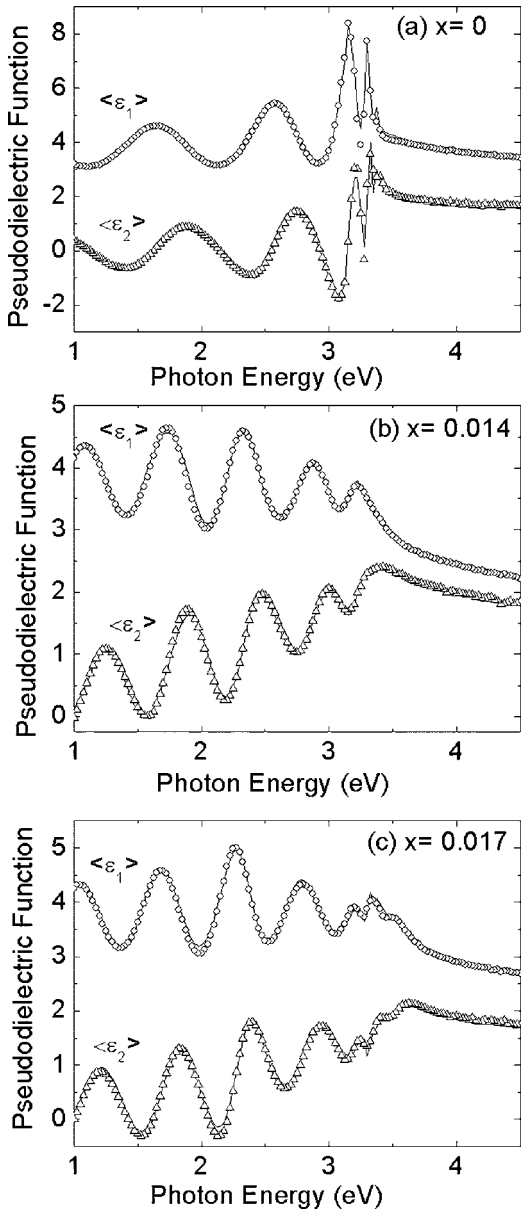

FIG. 4. The measured pseudodielectric function (discrete symbols) of $Zn_{1-x}Mn_xO$ [(a) $x=0.0$, (b) $x=0.014$, (c) $x=0.017$] measured at a 70° angle of incidence and its fitted curve (solid lines).

To take into account the excitonic effect for (Zn,Mn)O semiconductor, we adopted the Holden line-shape formula, which was derived from first-principle calculation by Tanguy[15] and Holden *et al.*[16]

The strong excitonic property of the E_0 gap modifies significantly the dielectric functions near the E_0 gap in ZnO. This phenomenon is typical in II-VI semiconductors, which have strong ionic characteristics in general. Using a Lorentzian approximation for line-shape broadening of both the excitonic states and the band edge, Holden *et al.* derived the dielectric function near a three-dimensional critical point (CP) modified by excitonic interaction using five parameters. The formula can be expressed by

$$\varepsilon(E) = \frac{A}{2E^2}\sum_{n=1}^{\infty}\left[g_{b,n}(E+i\Gamma_n) - g_{b,n}(i\Gamma_n)\right] + g_u(E+i\Gamma_0) - g_u(i\Gamma_0), \quad (1)$$

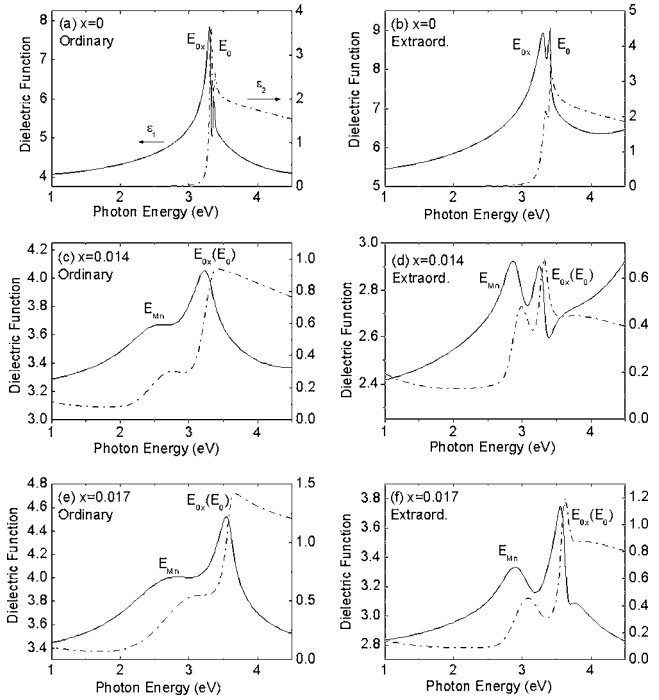

FIG. 5. The fitted layer dielectric function of $Zn_{1-x}Mn_xO$ {[(a) and (b)] $x=0.00$, [(c) and (d)] 0.014, [(e) and (f)] 0.017} thin film. The ordinary (extraordinary) dielectric function is the dielectric response when the electric field is perpendicular (parallel) to the growth axis. The Mn-related peak near 3 eV is identified as E_{Mn}.

$$g_{b,n}(\xi) = \frac{8R}{n^3}\left[\frac{E_0 - \frac{R}{n^2}}{\left(E_0 - \frac{R}{n^2}\right)^2 - \xi^2}\right], \tag{2}$$

$$g_u(\xi) = -\ln\left(\frac{E_0^2 - \xi^2}{R^2}\right) - \frac{1}{2}\sum_{n=1}^{\infty} g_{b,n}(\xi) - \pi\left[\cot\left(\frac{\pi\sqrt{R}}{\sqrt{E_0 - \xi}}\right) + \cot\left(\frac{\pi\sqrt{R}}{\sqrt{E_0 + \xi}}\right)\right], \tag{3}$$

where the parameters are the amplitude A, the CP energy E_0, the excitonic binding energy R, the broadening of the band gap Γ_0, and the broadening of the exciton Γ_{0x}. The E_0 band gap designates the fundamental interband transition between valence and conduction bands at Γ point in Brillouin zone. The energy and broadening of the nth exciton of E_0 gap is given by

$$E_{n,0}^{\mathrm{ex}} = E_0 - \frac{R}{n^2}, \tag{4}$$

$$\Gamma_n = \Gamma_0 - \frac{\Gamma_0 - \Gamma_0^{\mathrm{ex}}}{n^2}. \tag{5}$$

To accommodate the contributions from the electronic transitions at energies above the experimental energy range, we added an undamped harmonic oscillator model to Eq. (1),

$$\varepsilon(E) = \frac{A_1 E_1^2}{E_1^2 - E^2}. \tag{6}$$

TABLE I. The fitted thickness values of $Zn_{1-x}Mn_xO$ thin films. The numbers in the parentheses are uncertainties with 95% reliabilities.

$Zn_{1-x}Mn_xO$	Surface roughness layer (nm)	$Zn_{1-x}Mn_xO$ top layer (nm)	ZnO buffer layer (nm)
$x=0$	3.2(3.0)	321.9(6.0)	⋯
$x=0.014$	18.8(2.0)	421.0(3.0)	123.1(7.0)
$x=0.017$	11.6(1.5)	387.0(10.0)	152.1(3.0)

Here E_1 denotes the interband transition between valence and conduction bands along Λ line in the Brillouin zone.

In consistence with the absorption data of Figs. 1 and 3, the optical structure near 3 eV due to intra-d-shell transitions in Mn ions[12] is identified and was fitted assuming Gaussian lineshape. The Gaussian line shape is expressed as

$$\varepsilon_{\mathrm{Mn}} = \varepsilon_{1,\mathrm{Mn}} + i\varepsilon_{2,\mathrm{Mn}},$$

where

$$\varepsilon_{2,\mathrm{Mn}} = A_2 e^{-(E - E_{\mathrm{Mn}}/\Gamma_2)^2} + A_2 e^{-(E + E_{\mathrm{Mn}}/\Gamma_2)^2},$$
$$\varepsilon_{1,\mathrm{Mn}} = \frac{2}{\pi}\int_0^{\infty} \frac{\xi\varepsilon_{2,\mathrm{Mn}}(\xi)}{\xi^2 - E^2} d\xi, \tag{7}$$

where $E_{\mathrm{Mn}}(\Gamma_2)$ is the peak energy (the broadening) of the midgap peak. Our data and fitting showed that the binding energy decreased with increasing Mn composition. Mn-related crystalline disorder such as interstitials and precipitations may cause the decrease of the excition binding energy. The increase of broadening may be attributed partly to an inhomogeneous distribution of Mn ions.

Table I shows the fitted layer thicknesses. Table II shows the fitted band-gap parameters for the model of Holden *et al.* estimated from ellipsometric spectra. When Mn composition is very small, i.e., less than 2%, we cannot tell whether the E_0 band-gap energy increased or not with increasing Mn composition from Table II. Surprisingly, with 1% or 2% of incorporation of Mn into ZnO thin film, the broadening parameters Γ_0 and Γ_{0x} increased enormously compared to those of ZnO, suggesting that Mn atoms are strong perturbation for ZnO matrix. The exciton binding energy of ordinary dielectric function decreased with increasing Mn composition, whereas that of the extraordinary dielectric function was constant. We note that it is already shown in the absorption spectra of Fig. 1 that band gap increases with increasing Mn composition.

In Fig. 5, the E_{Mn} peak near 3 eV is Mn-related as was shown in the absorption spectra of Figs. 1 and 3. Kim and Park[5] also reported the Mn-related peak in (Zn,Mn)O using spectroscopic ellipsometry. In their work, they showed clearly the Mn-related peak in the pseudodielectric function spectra because the interference below band edge was negligible due to rough interface between (Zn,Mn)O and the sapphire substrate. The enormous broadening of Γ_0 and Γ_{0x} of (Zn,Mn)O is in contrast to the small increase of that of (Zn,Mg)O thin films grown on (0001) sapphire.[13] The ellipsometric spectra of $Zn_{0.83}Mg_{0.17}O$ could resolve detailed ex-

TABLE II. The fitted band-gap and exciton parameters of E_0 and E_1 band gaps, and the parameters of the Mn-related midgap peak. Here A is the amplitude, E_0 is the energy, R is the binding energy, and Γ_0 (Γ_{0x}) is the broadening of E_0 gap (E_{0x} exciton) peak. A_1 and E_1 denote the amplitude and energy of E_1 band gap, respectively. A_2, E_{Mn}, and Γ_2 denote the amplitude, energy, and broadening of Mn-related gaussian peak, respectively. The numbers in the parentheses are uncertainties with 95% reliabilities.

	A	E_0 (eV)	R (eV)	Γ_0 (eV)	Γ_{0x} (eV)	$A1$	E_1 (eV)	$A2$	E_{Mn} (eV)	Γ_2 (eV)
$x=0$	7.53	3.378	0.060	0.001	0.058	145.7	8.92	—	—	—
$E\perp c$	(0.14)	(0.004)	(0.002)	(0.02)	(0.04)	(1.0)	(0.02)			
$E\|c$	10.07	3.410	0.070	0.004	0.024	138.8	7.37	—	—	—
	(1.44)	(0.004)	(0.002)	(0.004)	(0.002)	(0.4)	(0.02)			
$x=0.014$	3.53	3.30	0.050	0.089	0.147	151.8	9.55	0.19	2.69	0.599
$E\perp c$	(0.41)	(0.08)	(0.04)	(0.02)	(0.08)	(4.6)	(1.2)	(0.02)	(0.06)	(0.118)
$E\|c$	2.08	3.39	0.072	0.314	0.077	54.3	7.00	0.28	2.96	0.252
	(0.62)	(0.04)	(0.02)	(0.10)	(0.04)	(2.0)	(1.0)	(0.03)	(0.04)	(0.074)
$x=0.017$	5.55	3.59	0.035	0.058	0.114	118.4	9.00	0.43	3.06	0.980
$E\perp c$	(0.88)	(0.07)	(0.03)	(0.01)	(0.15)	(14.4)	(2.0)	(0.05)	(0.1)	(0.160)
$E\|c$	4.54	3.69	0.072	0.127	0.068	145.5	10.9	0.32	3.07	0.398
	(0.14)	(0.07)	(0.08)	(0.08)	(0.05)	(6.0)	(2.0)	(0.10)	(0.04)	(0.130)

citonic structures associated with E_0 because of their sharp line shapes.[13] We note that we also measured the pseudodielectric functions for (Zn,Mn)O thin films with higher Mn compositions ($x \geqslant 0.023$) which were grown on sapphire substrate with and without GaN buffer layer. However, we could not fit the dielectric function using the model of Holden *et al.*. With increasing Mn composition, the crystallinity of (Zn,Mn)O decreases and Mn-related defects increases. This may disrupt excitions and model of Holden *et al.* will not be effective any more. Note that model of the Holden *et al.* assumes strong ionic properties and that the E_0 and E_1 gap features are always accompanied with their corresponding exciton partners in the line-shape model.

IV. CONCLUSIONS

(Zn,Mn)O thin films with/without GaN buffer layers by using rf sputtering deposition in a gas mixture of Ar and N_2 were grown. We measured the optical absorption spectra of (Zn,Mn)O thin films. We found that the optical gap energy decreased and the Mn-related peak intensity decreased with increasing N_2 flow rate. Using spectroscopic ellipsometry, we measured the pseudodielectric functions of (Zn,Mn)O. Using model of the Holden *et al.*, we fitted the dielectric function and determined the band-gap parameters as a function of Mn composition. We also found a 3 eV peak which was attributed to intra-*d*-shell transitions of Mn^{2+} ions. Our study showed the evolution of the optical properties with increasing Mn composition: The E_0 band-gap energy did not change appreciably up to 2% Mn, and the broadenings increased enormously even for less than 2% of Mn composition. We conclude that the incorporation of Mn ions into the ZnO thin films is a strong perturbation because the broadening of the E_0 and E_{0x} peaks increased enormously with the addition of Mn ions.

ACKNOWLEDGMENTS

This work was supported in part by the Air Force Office of Scientific Research (Dr. G. L. Witt). One of the authors (H.L.) was supported in part by Kyung Hee University Fund during 2004-2005. One of the authors (H.L). thanks S. Chevtchenko for taking part of optical absorption data.

[1] T. Dietl, H. Ohno, F. Matsukura, J. Cibert, and D. Ferrand, Science **287**, 1019 (2000).
[2] T. Fukumura, Z. Jin, A. Ohtomo, H. Koinuma, and M. Kawasaki, Appl. Phys. Lett. **75**, 3366 (1999).
[3] A. Tiwari, C. Jin, A. Kvit, D. Kumar, J. F. Muth, and J. Narayan, Solid State Commun. **121**, 371 (2002).
[4] T. D. Kang, H. Lee, W.-I. Park, and G.-C. Yi, Thin Solid Films **455/456**, 609 (2004).
[5] K. J. Kim and Y. R. Park, J. Appl. Phys. **94**, 867 (2003).
[6] Q. Wang, Q. Sun, P. Jena, and Y. Kawazoe, Phys. Rev. B **70**, 052408 (2004).
[7] D. C. Look and B. Claflin, Phys. Status Solidi B **241**, 624 (2004).
[8] A. Tsukazaki *et al.*, Nat. Mater. **4**, 42 (2005).
[9] C. Liu *et al.*, Superlattices Microstruct. **39**, 124 (2006).
[10] Ü. Özgür *et al.*, J. Appl. Phys. **98**, 041301 (2005).
[11] V. Avrutin *et al.*, Superlattices Microstruct. **39**, 291 (2006).
[12] Z.-W. Jin, Y.-Z. Yoo, T. Sekiguchi, T. Chikyow, H. Ofuchi, H. Fujioka, M. Oshima, and H. Koinuma, Appl. Phys. Lett. **83**, 38 (2003).
[13] R. Schmidt *et al.*, Appl. Phys. Lett. **82**, 2260 (2003).
[14] *Handbook of Optical Constants of Solids III*, edited by E. D. Palik (Academic, New York, 1998), pp. 675 and 676.
[15] C. Tanguy, Phys. Rev. Lett. **75**, 4090 (1995).
[16] T. Holden, P. Ram, F. H. Pollak, J. L. Freeouf, B. X. Yang, and M. C. Tamargo, Phys. Rev. B **56**, 4037 (1997).